

LA-UR-18-26989

Approved for public release; distribution is unlimited.

Title: Beam Profile Measurements at the DARHT II Accelerator Exit

Author(s): Schulze, Martin E.
Ekdahl, Carl August Jr.
Johnson, Jeffrey B.
Mccrady, Rodney Craig
Russell, Steven John
Carlson, Carl A.

Intended for: Report

Issued: 2018-07-26

Disclaimer:

Los Alamos National Laboratory, an affirmative action/equal opportunity employer, is operated by the Los Alamos National Security, LLC for the National Nuclear Security Administration of the U.S. Department of Energy under contract DE-AC52-06NA25396. By approving this article, the publisher recognizes that the U.S. Government retains nonexclusive, royalty-free license to publish or reproduce the published form of this contribution, or to allow others to do so, for U.S. Government purposes. Los Alamos National Laboratory requests that the publisher identify this article as work performed under the auspices of the U.S. Department of Energy. Los Alamos National Laboratory strongly supports academic freedom and a researcher's right to publish; as an institution, however, the Laboratory does not endorse the viewpoint of a publication or guarantee its technical correctness.

Beam Profile Measurements at the DARHT II Accelerator Exit

Martin Schulze, Carl Ekdahl, Jeffrey Johnson, Rod McCrady and Steven Russell

J-5 – Los Alamos National Laboratory

Carl Carlson

National Security Technologies, LLC

Abstract

Measurements of the beam profile at the exit of the DARHT II accelerator have been made. The 1.65-kA, 17-MeV DARHT-II linear induction accelerator [1] is unique in that its beam pulse has a long, 1.6-ns flattop during which the kinetic energy varies by less than $\pm 2\%$. Four short pulses are selected out of this long pulse in the downstream transport [2], and these are converted to bremsstrahlung for multi-pulse flash radiography of high explosive driven hydrodynamic experiments. The objective of the measurements was to demonstrate the capability to make these measurements with a long beam pulse of high intensity. Many observations can be made on the basis of these measurements. These are described herein.

Introduction

Measurements of optical transition radiation (OTR) or Cherenkov radiation from a beam intercepting target are common methods used at DARHT to observe the beam profile. Measurements of the beam profile at the accelerator exit had not been made previously on the full energy DARHT II accelerator due to concerns of beam induced damage to the target resulting in contamination of the accelerator. Prior measurements had been made at the accelerator exit on a scaled DARHT II accelerator (8 MeV and 1.0 kA) [3]. Beam profile measurements of the four short pulses have also been made.

The objective of the measurement was to obtain a baseline measurement of the beam profile at the accelerator exit in order to compare with model predictions and provide some information of the initial beam conditions for downstream transport (DST) simulations. By demonstrating the feasibility of the measurement, additional measurements may be performed in the future to better understand the beam properties.

Accelerator Configuration and Layout

The DST layout for these measurements is shown in Figure 1. This corresponds to the Axis 2 configuration for mode 1 operations with the beam stop in. Prior to making these measurements the injector was modified to shorten the pulse length reducing the risk of damage to the OTR target at Station A. At this time a new cathode was also installed. The actual beam pulse length is set with the injector crowbar. The Station A target is a .002" Ti foil at a 45° angle to the beam. A PIMAX2 camera is focused on the beam image using a 45° mirror resulting in an image of the actual beam shape. All measurements were made with solenoid S1 off.

Station A Optics

The beam exiting the accelerator is transported to the beam stop and S2 is used to expand the beam size on the beam stop to reduce the power density. The optics were investigated for a variety of initial conditions using TRANSPORT. The normalized beam emittance is assumed to be $800 \pi(\text{mm-mrad})$. A variety of initial beam conditions were studied and the S2 solenoid is operated at its nominal field corresponding to 275 A. We can simulate the effect of the foil using TRANSPORT which does include space charge. To simulate the foil, we add multiple Coulomb scattering (MCS) in the foil to the beam angular

distribution in quadrature and subtract the beam energy loss at the location of the Station A target. The results are shown in Figure 2 corresponding to an initial rms beam size of 1.0 cm. We see that the beam size on the dump is larger in the presence of the Station A foil. This simulation does not include the space charge neutralization in the Ti foil which is smaller than the effect of MCS.

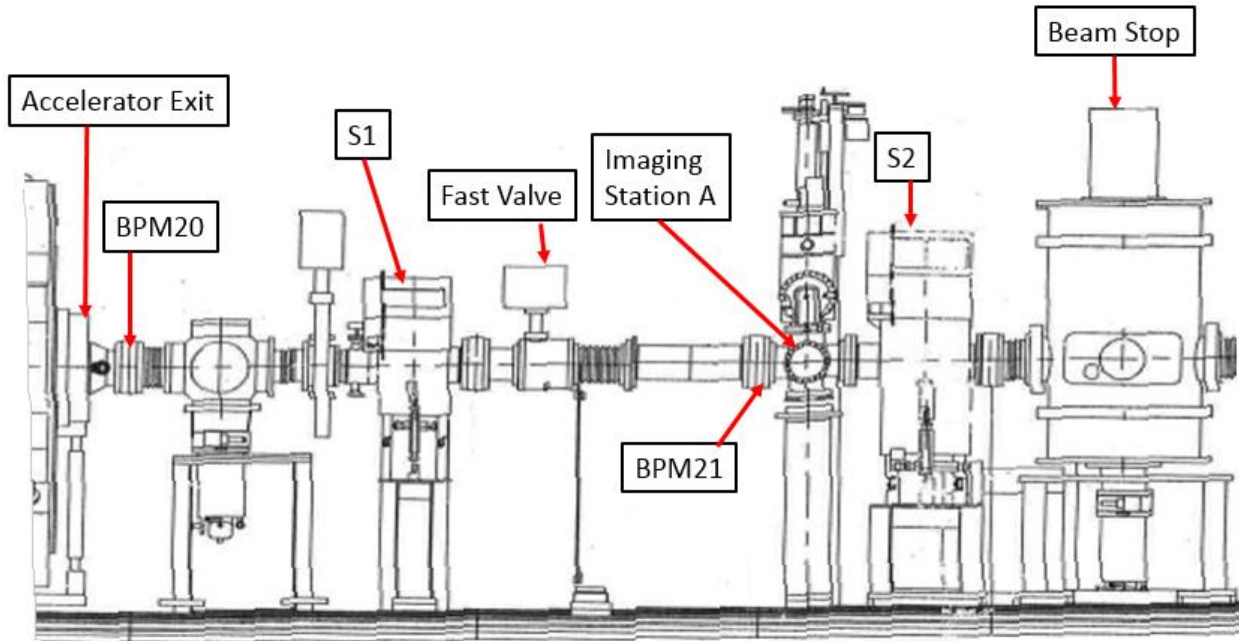


Figure 1: DST layout in Mode 1 showing locations of key components

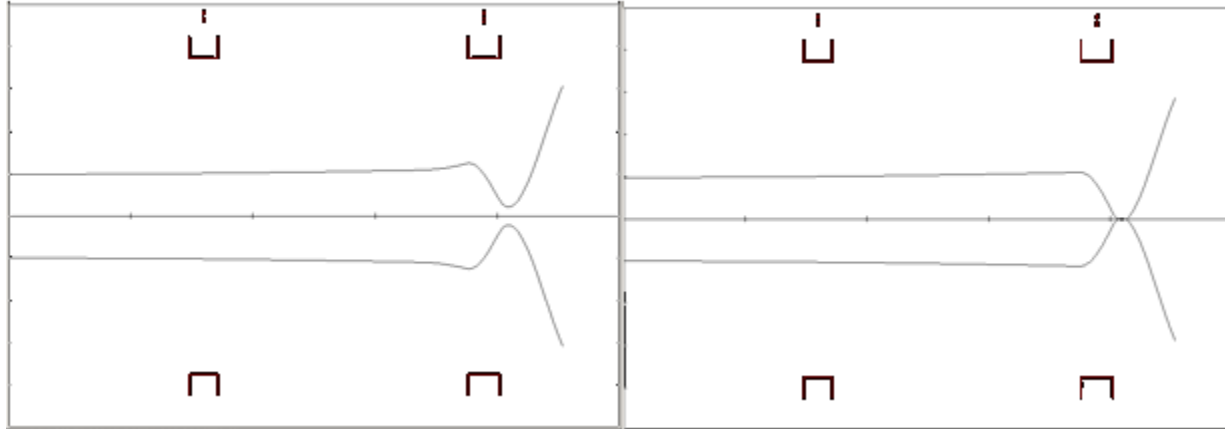


Figure 2: Horizontal (top) and vertical (bottom) rms beam envelopes with (left) and without (right) the Station A target for an initial rms beam size of 1.0 cm.

Measurements

Beam profile measurements were made at different times in the pulse as the pulse length was lengthened. Initially, the pulse length was as short as possible to both establish the camera timing and demonstrate the survival of the Ti foil. Figure 3 shows the beam energy and current as a function of time along with the six times at which the measurements were made. These times are 2.47, 2.57, 2.67, 2.77, 2.87, and 2.97 μ s. Typically, the P1 time for a hydrotest occurs at 2.47 μ s and most Station C studies are at 2.8 μ s.

Figures 4a-d show the beam image at four different times as indicated. The beam shape is clearly elliptical which was unexpected. This ellipticity requires a quadrupole field or a field gradient. This is addressed later in this document. The dark lines in the images are a mesh screen inside the vacuum window.

Figure 5 shows the measured full width at half maximum (FWHM) of the integrated beam distribution along both axes for all of the shots taken with the nominal tune. As seen in the figure there is very little variation in the spot size time outside of some statistical variation.

Figures 6 and 7 show lineouts of the beam profile at 2.67 and 2.97 μs respectively. The lineouts suggest the beam distribution is very uniform. This suggests very little emittance growth since the initial beam distribution at the cathode is also uniform. This is consistent with the findings of Ekdahl et al. [4].

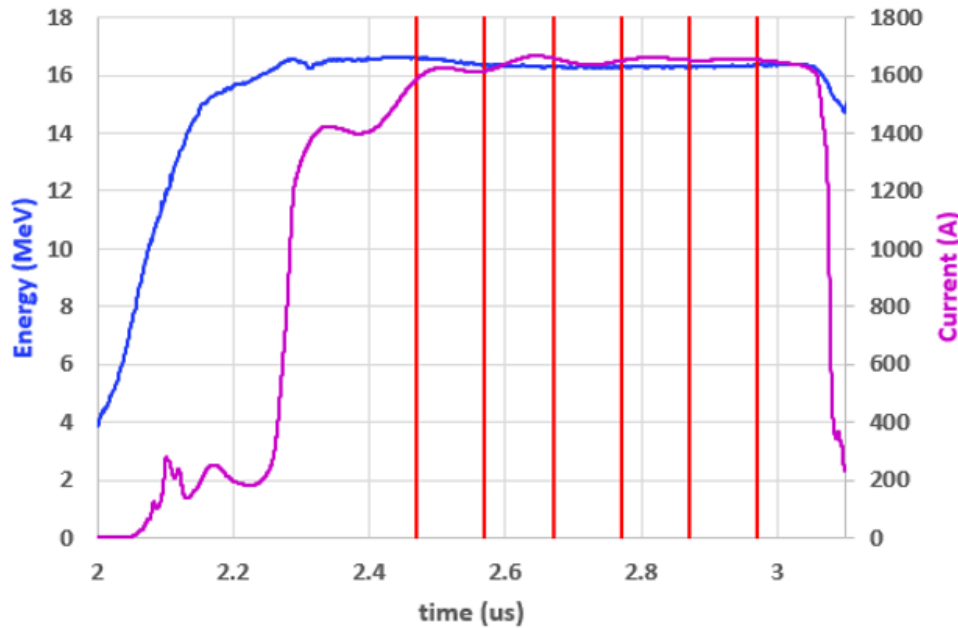


Figure 3: Beam energy (blue) and current (purple) as a function of time along with the times at which beam profile measurements were made.

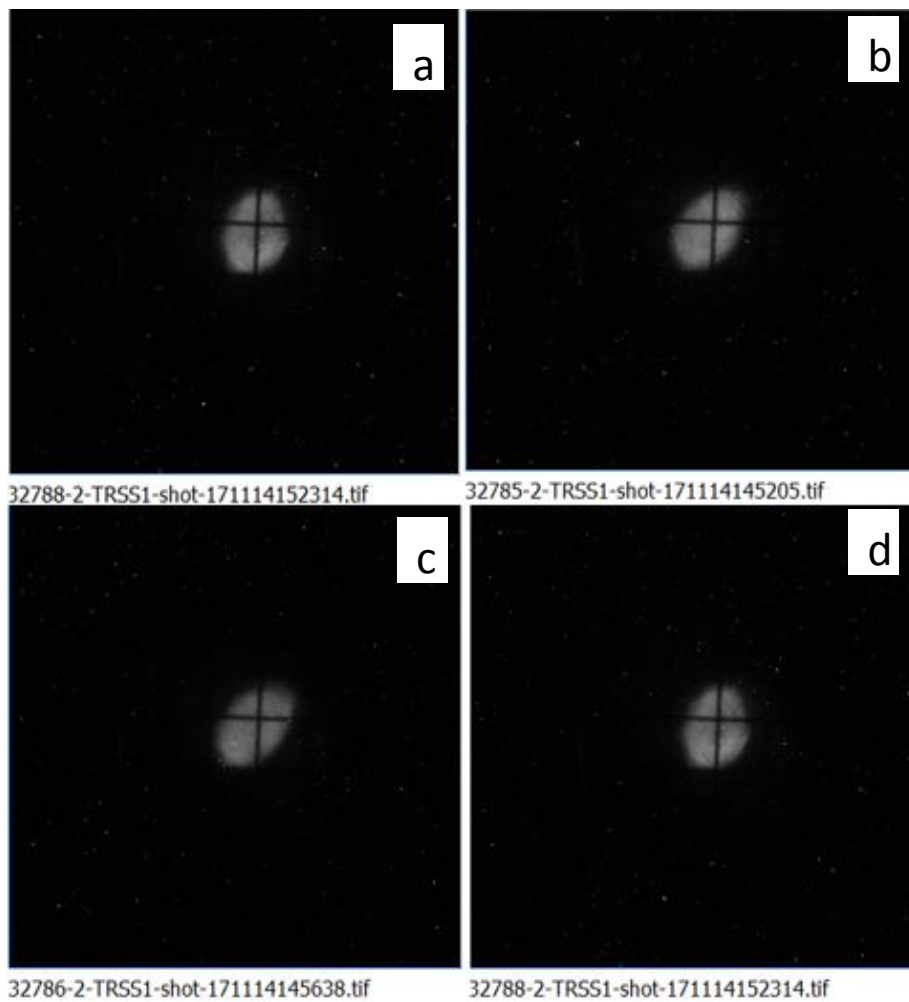


Figure 4: Measured beam profiles at (a) 2.67 μ s, (b) 2.77 μ s, (c) 2.87 ns and (d) 2.97 μ s

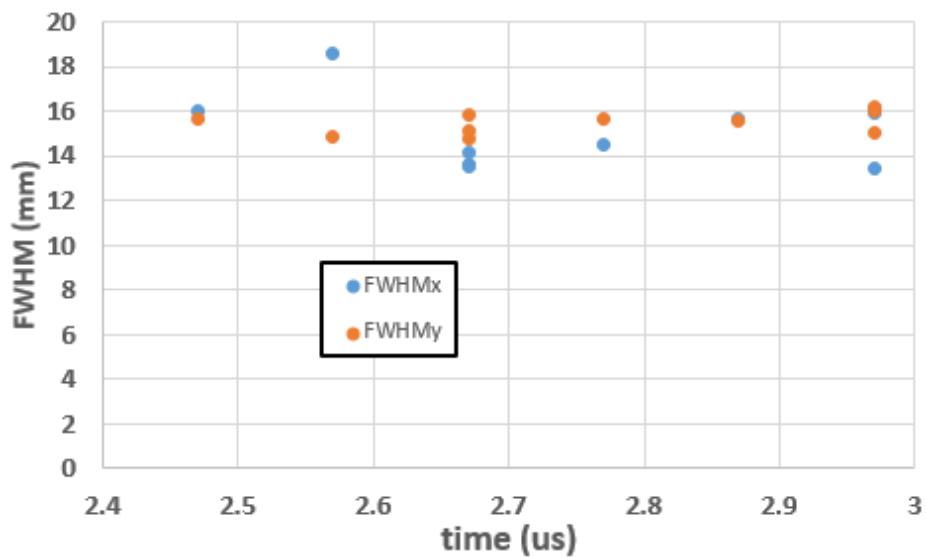
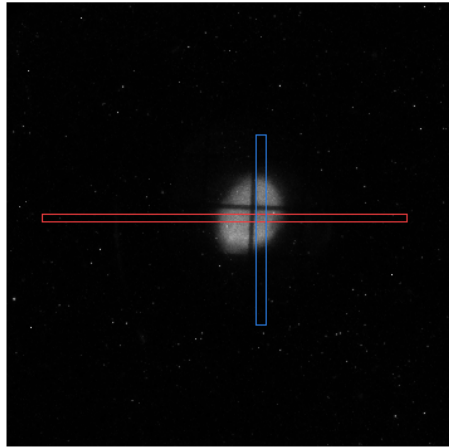


Figure 5: Measured FWHM for all shots taken with the nominal tune



32784-2-TRSS1-shot-171114144227.tif

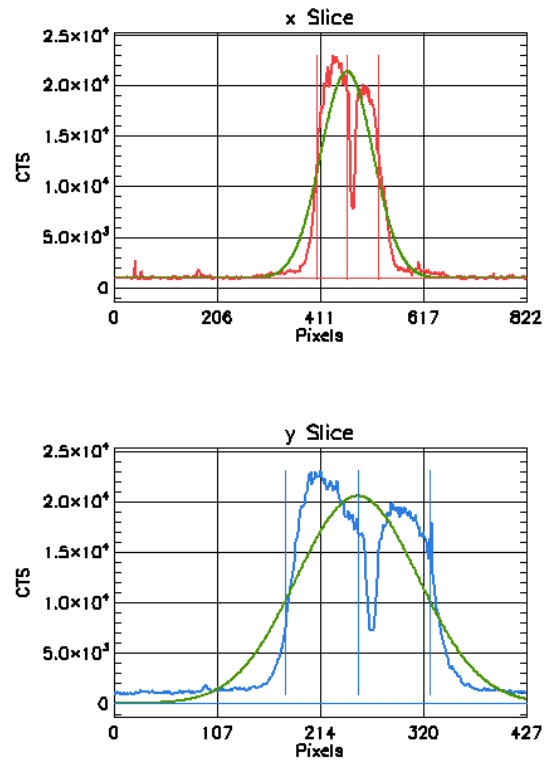
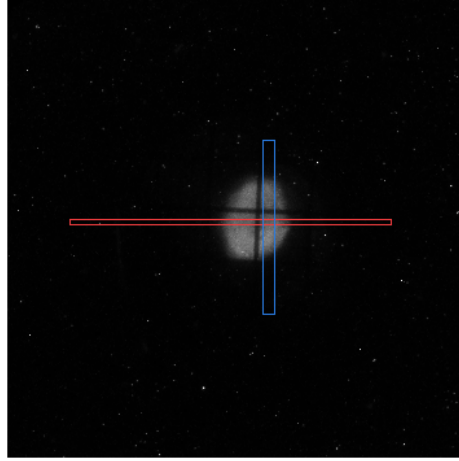


Figure 6: Lineouts of beam profile at 2.67 μ s. The red and blue lineouts correspond to the horizontal and vertical planes respectively. The green curve is a Gaussian distribution with the same FWHM.



32788-2-TRSS1-shot-171114152314.tif

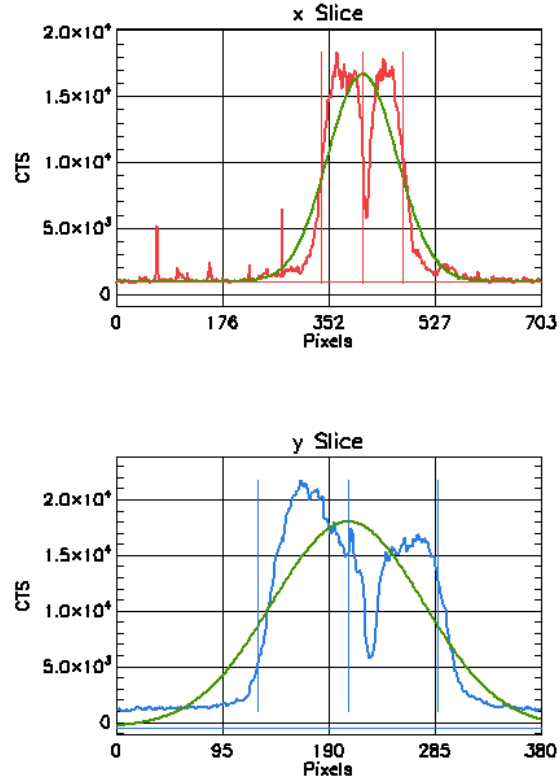


Figure 7: Lineouts of beam profile at 2.97us. The red and blue lineouts correspond to the horizontal and vertical planes respectively. The green curve is a Gaussian distribution with the same FWHM.

Comparison with Simulations

One of the main objectives in making these measurements was to obtain baseline measurements of the beam profile at or near the accelerator exit. Figure 8 shows a simulation of the beam envelope in the accelerator. The beam envelope radius at Station A ($z=5370$ cm) is about 1.2 cm. The normalized beam emittance in Figure 8 is $210 \pi(\text{mm-mrad})$. This is consistent with the measurements shown above. Unfortunately, we cannot make any definitive statements regarding the beam at the accelerator exit as demonstrated in Figures 9 and 10. However it is likely that the normalized emittance is less than $1000 \pi(\text{mm-mrad})$ because the beam size is greater than 1.5 cm for all initial envelope radii although a slightly converging beam may be smaller. For the smaller normalized emittance of $500 \pi(\text{mm-mrad})$, it appears that a wide range of initial beam emittances are consistent with the measured beam profile.

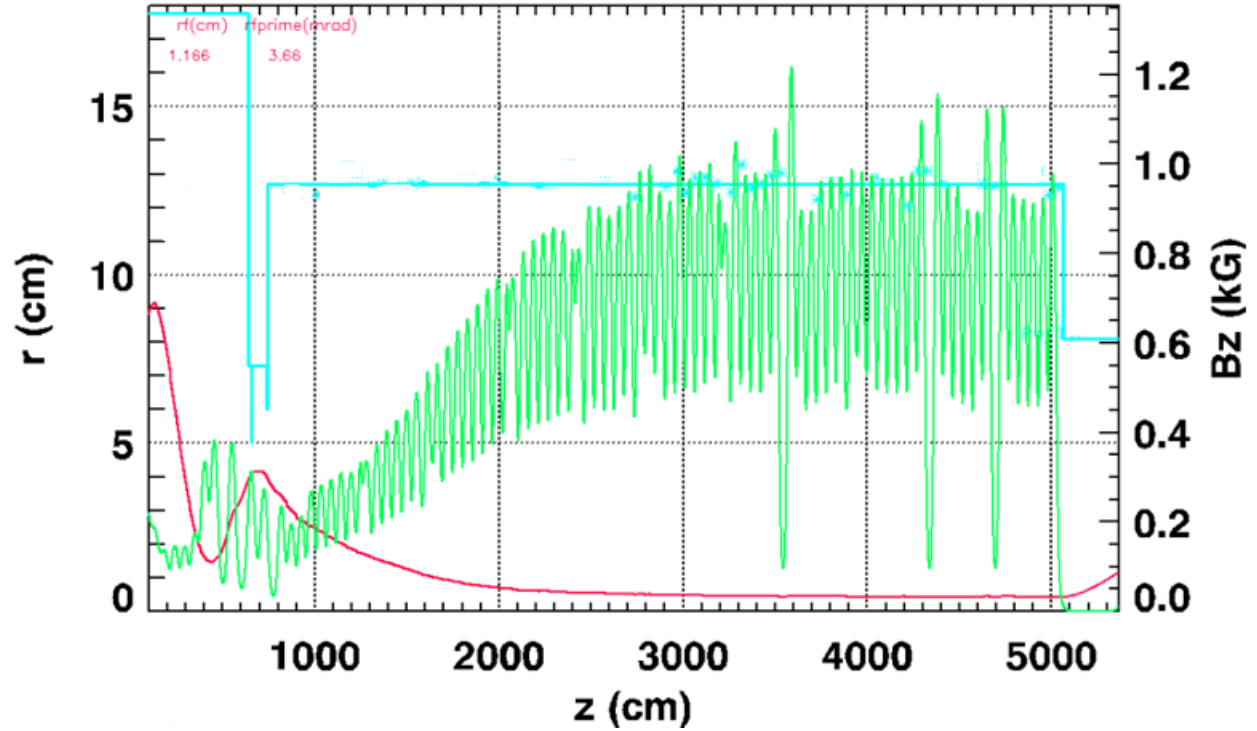


Figure 8: Beam envelope radius (red) in the accelerator along with the magnetic field (green) and the radius of the beam tube (light blue).

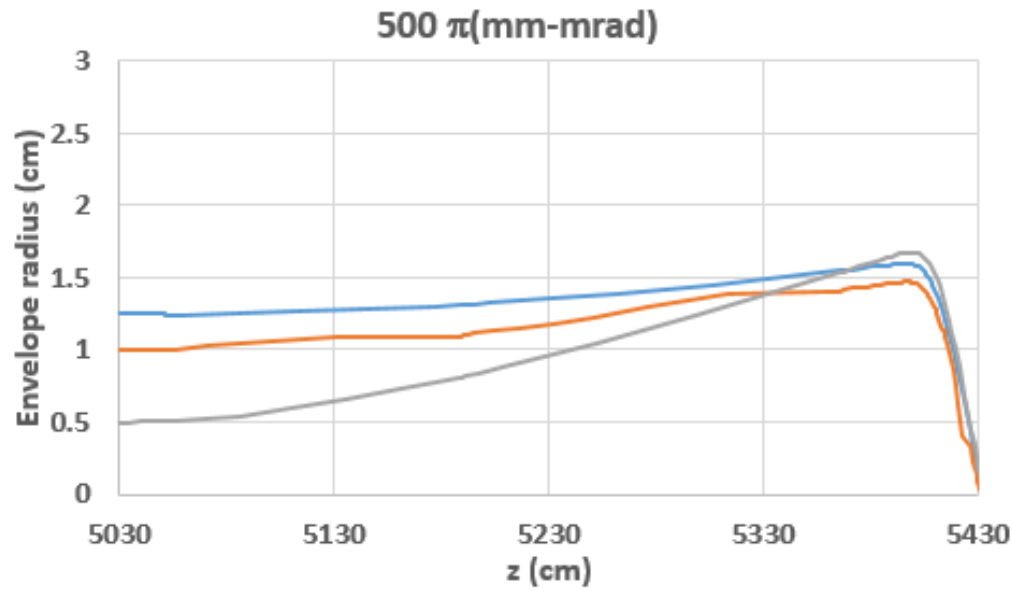


Figure 9: Beam profile for three different initial beam sizes at the accelerator exit for a normalized n emittance of $500 \pi(\text{mm-mrad})$. The three curves correspond to beam sizes of 0.5 cm (grey), 1.0 cm (orange) and 1.25 cm (blue). The initial beam convergence angle is zero for all simulations.

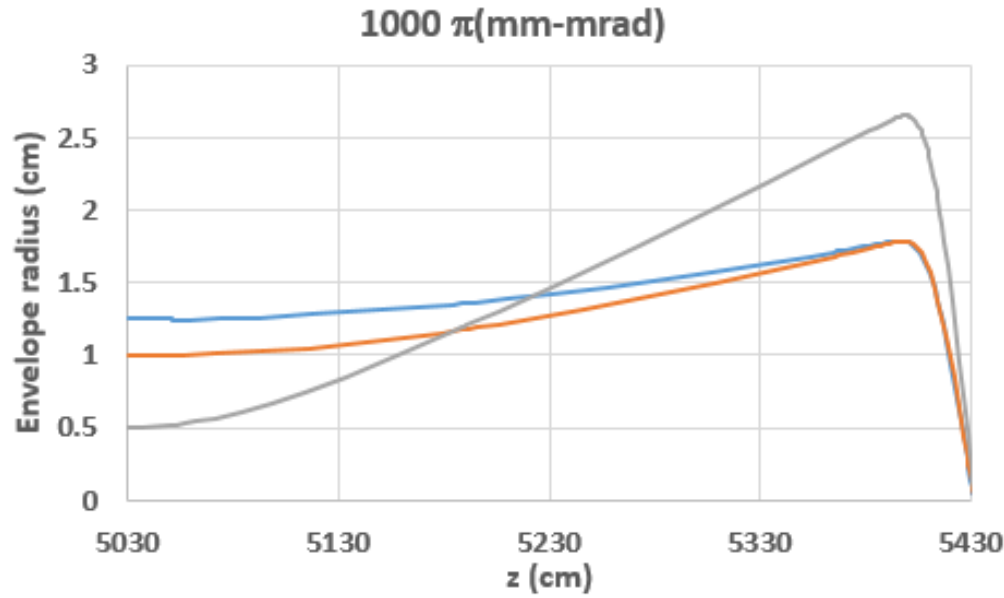


Figure 10: Beam profile for three different initial beam sizes at the accelerator exit for a normalized emittance of 1000π (mm-mrad). The three curves correspond to beam sizes of 0.5 cm (grey), 1.0 cm (orange) and 1.25 cm (blue). The initial beam convergence angle is zero for all simulations.

Foil Heating

Station A measurements of the beam profile had not previously at full energy and current due to concerns regarding beam heating of the target and potential damage to the accelerator. Preliminary estimates of the foil heating showed that for short pulses (200 ns or less) the foil should easily withstand spot sizes of 0.5 cm radius. Initial measurements with a very short pulse showed the beam size to be uniform with an area corresponding to a circle of about 0.86 cm radius. After inspection of the foil showed no damage, it was decided to further increase the pulse length. After three shots and the pulse length shown in Figure 3, a “dead” spot was observed in the beam image. Visual inspection did not show any damage and four more shots were fired with different beam steering. At this point, visual inspection clearly indicated a distortion on the foil surface as shown in Figure 11. Titanium has a melting point of 1668°C as well as a phase transition at 868°C. Thermal analysis of the beam heating of the foil was performed for several different pulse lengths and different beam radii as shown in Figure 12. A uniform beam distribution was assumed in the calculation. As discussed above, the beam distribution is approximately uniform with an area equivalent to a round beam of 0.86 cm radius. It is clear from Figure 12 that the distortion of the foil is a result of the phase transition. Based on the calculations shown in Figure 12 and the measured beam spot size, further measurements at Station A can be pursued at pulse lengths of about 200 ns shorter.



Figure 11: Picture of Station A Ti foil target showing phases transition in center after removal from beam line.

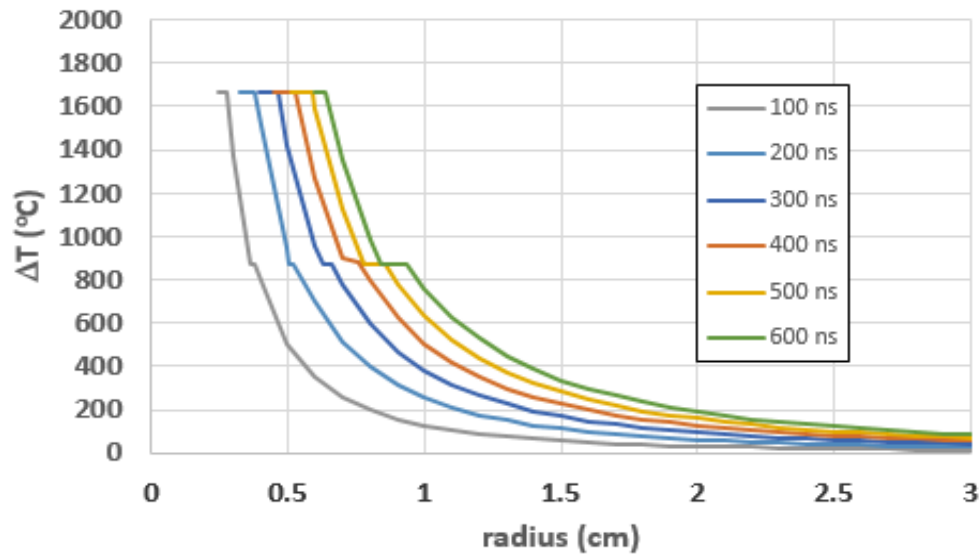


Figure 12: Thermal analysis of foil temperature rise due to beam heating.

Ellipticity

The source of the elliptical beam profile is not immediately obvious. Beam profile measurements were made for different settings of the first three accelerator solenoids (cell solenoids 7, 8 and 9). Figures 13a-c shows the measured beam profile for three different settings of cell solenoids 7, 8 and 9. Figures 13a-c clearly show that as the magnetic field is increased to rotation of the distribution changes. This strongly indicates that the beam distribution is already elliptical prior to these solenoids.

Two possible sources of the elliptical beam profile are (1) a stray field with a linear gradient and (2) a beam traversing the A-K gap at an angle. We know that there is a very significant stray field in the injector caused by the vertical stalk providing voltage to the injector. The measured beam position in the injector is over 10 mm off axis. This alone will cause the beam to traverse the A-K gap at an angle.

The effect of a stray field with a linear gradient is examined analytically. A round beam of 3.0 cm diameter is transported through a 10 cm field with a .333 G/cm gradient. The resulting beam profile is calculated after an additional drift of 10 cm. The beam parameters are presented in Table 1. Figure 14 show the transformation of a round beam (blue) after traversing the region of the field gradient and a 10 cm drift. The change in the shape is evident.

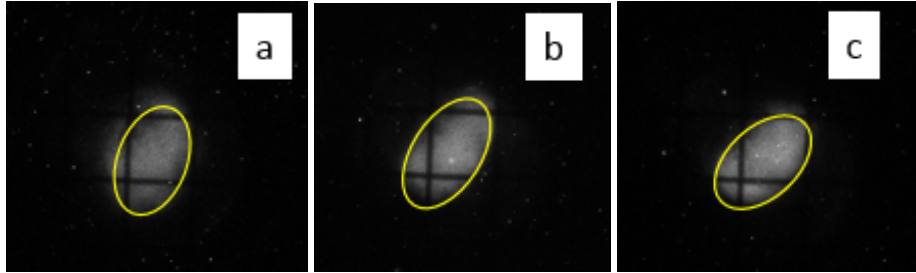


Figure 13: Beam profile for different settings of cell solenoids 7, 8 and 9. Figure 13b corresponds to the nominal setting of these solenoids while Figure 13a and 13c are for settings 5% lower and 5% higher respectively. The yellow ellipses have been added to enhance the outline of the distribution.

Table 1: Parameters used to simulate effect of stray field

Energy	2.1 MeV
Momentum	2.56 MeV/c ²
Length	10 cm
Field	0.333 G/cm
Angle	23.42 mrad

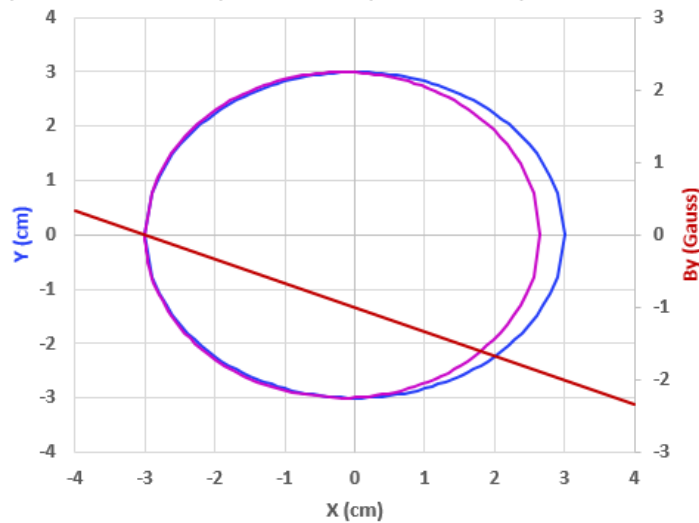


Figure 14: Simulation of the effect of a field gradient of 0.333 G/cm on the shape of the beam. The blue trace is the circular beam entering the region of the field gradient. The purple curve is the beam after traversing the field and drifting another 10 cm. The red curve is the vertical field.

Conclusions

The first measurements of the beam profile at the accelerator has provided important information about the DARHT II beam. The beam distribution is very uniform suggesting little emittance growth in the accelerator. The elliptical beam profile is probably due to stray fields in the injector region. The beam size and shape do not appear to vary significantly as a function of time. Future measurements should be made with a shorter pulse to avoid damage to the foil.

References

- [1] Carl Ekdahl, et al., "Electron beam dynamics in the long-pulse, high-current DARHT-II linear induction accelerator", in Proc. 2009 Particle Accelerator Conf., pp. 3080-3084 (May 2009).
- [2] Martin Schulze, et al., "Commissioning the DARHTII Accelerator Downstream Transport and Target", in Proc. 2008 Linear Accel. Conf., pp. 427-429 (Sept. 2008).
- [3] Carl Ekdahl, et al., "Commissioning the DARHT II Scaled Accelerator", in Proc. 2007 Particle Accelerator Conf., pp. 2373-2375 (May 2007).
- [4] Carl Ekdahl et al., "Emittance Growth in the DARHT-II Linear Induction Accelerator", IEEE Transactions on Plasma Science, Vol. 45, No 11, pp. 2962-2973. (November 2017).